
ENABLING WEAK CLIENT PARTICIPATION VIA ON-DEVICE KNOWLEDGE DISTILLATION IN HETEROGENEOUS FEDERATED LEARNING

Jihyun Lim
Inha University
wlguslim@inha.edu

Junhyuk Jo
Inha University
911whwnsgur@inha.edu

Tuo Zhang
University of Southern California
tuo Zhang@usc.edu

Salman Avestimehr
University of Southern California
avestime@usc.edu

Sunwoo Lee
Inha University
sunwool@inha.ac.kr

March 17, 2025

ABSTRACT

Online Knowledge Distillation (KD) is recently highlighted to train large models in Federated Learning (FL) environments. Many existing studies adopt the logit ensemble method to perform KD on the server side. However, they often assume that unlabeled data collected at the edge is centralized on the server. Moreover, the logit ensemble method personalizes local models, which can degrade the quality of soft targets, especially when data is highly non-IID. To address these critical limitations, we propose a novel on-device KD-based heterogeneous FL method. Our approach leverages a small auxiliary model to learn from labeled local data. Subsequently, a subset of clients with strong system resources transfers knowledge to a large model through on-device KD using their unlabeled data. Our extensive experiments demonstrate that our on-device KD-based heterogeneous FL method effectively utilizes the system resources of all edge devices as well as the unlabeled data, resulting in higher accuracy compared to SOTA KD-based FL methods.

1 Introduction

Federated Learning (FL) [1] is a practical learning method to utilize the data collected on-the-fly at the edge. Recently, with the rapid advancement of edge device system efficiency, various large-scale on-device learning scenarios are being considered, such as multi-task transfer learning [2], sharpness-aware minimization [3], and even Large Language Model (LLM) fine-tuning [4]. These on-device learning studies commonly assume that the devices are homogeneous and thus all the devices can equally contribute to the model training. However, FL environments often consist of heterogeneous edge devices such as mobile phones or IoT devices. Therefore, to exploit the ever-increasing big data collected at the edge, it is imperative to develop a new FL method that can fully utilize heterogeneous system resources. Several recent studies tackle the system heterogeneity issue in FL by employing partial model training scheme [5, 6, 7, 8, 9, 10]. However, they enforce clients with weak resources to train only a subset of the target model’s layers or channels, significantly harming the freedom of model design. More recent works utilize Knowledge Distillation (KD) [11]. They commonly use a logit ensemble method instead of directly aggregating the local models to reduce the KD’s communication cost in FL environments [12, 13]. In our empirical study, however, we find that the logit ensemble fails to provide sufficiently accurate soft targets when the data distribution is highly non-IID. Although a large amount of public data is available, KD with such inaccurate soft targets negatively impacts the efficiency of knowledge transfer. Some others utilize unlabeled extra data to train the target model on the server side [14, 15]. This approach assumes that unlabeled data generated on edge devices is aggregated on the server and utilized for centralized training, raising privacy concerns.

In this paper, we propose a novel heterogeneous FL method that utilizes unlabeled data at the edge to overcome the limitations of logit ensemble methods and server-side model training approaches. Specifically, we introduce a KD-based FL method that jointly utilizes additional system resources on strong devices and unlabeled local data by combining auxiliary model training and on-device KD. The core principle behind our method is that a small auxiliary model first learns global knowledge through standard model aggregation and then helps the training of the large target model by utilizing system resources and unlabeled local data on strong devices. When transferring global knowledge from the auxiliary model to the target model, only a subset of clients with sufficiently strong system resources participate in the KD process. This heterogeneous approach allows all the clients effectively join the training exploiting their own resources and local data.

Compared to logit ensemble-based KD, our method has two strong benefits as follows. First, our approach ensures accurate soft targets for the KD process. By aggregating the small auxiliary models across the clients, the local knowledges are directly merged into a single point, and it results in making the quality of the soft targets remarkably improved compared to the logit ensemble. Second, our approach does not require the server to have sufficiently strong system capability nor the unlabeled data to be centralized on the server in advance. By offloading the KD workload to the strong devices, the model can learn from the local data regardless of whether it is labeled or not. Moreover, as more clients join the training, our approach allows the model to learn from more unlabeled data, likely improving the model accuracy.

We evaluate the performance of our proposed method across various machine learning benchmarks: CIFAR-10 [16], CIFAR-100 (fine-tuning), FEMNIST [17], IMDB reviews [18], and Google Speech Commands [19]. Our extensive experiments demonstrate that the proposed method outperforms SOTA KD-based FL methods under highly non-IID conditions. We also theoretically analyze the generalization bound for the proposed method. The contributions of our work are summarized below.

- We explain and empirically prove the fundamental limitations of the logit ensemble-based Knowledge Distillation especially when the data is strongly non-IID.
- Our study demonstrates how to harmonize online Knowledge Distillation with FL to better utilize unlabeled data collected at the edge on-the-fly.
- We discuss how to exploit heterogeneous system resources in realistic FL environments via selectively offloading the distillation workload to the edge.
- Our study presents an extensive comparative analysis, demonstrating that the proposed method achieves superior soft target quality, resulting in higher accuracy.

2 Related Works

2.1 Heterogeneous Federated Learning

In realistic FL environments, some devices may not efficiently train large models or even cannot put them in their memory space. In this case, there are two options: employ a small model giving up the learning capability or keep using the large model giving up the private data owned by the weak devices. One promising solution to this system heterogeneity issue is partial model training method [5, 6, 7, 8, 9, 10, 20]. While these methods alleviate the workload for some clients, they do not consider independent model architectures across clients.

Another promising approach is heterogeneous model approximation method. Some recent works allow clients to reduce the model size according to their system capability [21, 22, 23, 24]. However, the low-rank model approximation causes a non-negligible extra computational cost. Additionally, the local models cannot be directly aggregated because each one may be approximated to a different rank.

2.2 Knowledge Distillation in Federated Learning

Table 1 summarizes the recently proposed KD-based FL methods. First, there are two homogeneous FL methods: FedAvg and MOON [25]. Neither of them considers the newly collected unlabeled data or utilizes KD.

Logit Ensemble – KD has been widely used in recent FL studies with a goal of either improving the model accuracy or training a large model. Federated KD proposed in [12] directly exchanges the soft targets across the server and the clients instead of exchanging the model parameters. DS-FL proposed in [13] exchanges only the soft targets under a strong assumption that the unlabeled data is available for all individual clients. FedMD [26] transfers knowledge by leveraging the fine-tuning mechanism. These methods commonly aggregate the local models’ output logits at the server and broadcast them to the clients. This approach significantly reduces the communication cost; however, the accuracy

Table 1: The configurations of SOTA FL methods.

Method	Server Model	Exchange	Additional Data / Labeled	KD
FedAvg	=client	model	No / N/A	N/A
MOON	=client	model	No / N/A	N/A
FD	N/A	logits	No / N/A	device
DS-FL	N/A	logits	Yes / No	device
FedMD	N/A	logits	Yes / Yes	device
FedDF	=client	model	Yes / No	server
FedGEMS	> client	logits	Yes / Yes	both
FedGKT	> client	model+logits	No / N/A	both
Fed-ET	> client	model+logits	Yes / No	server
Ours	N/A	model	Yes / No	device

drop is significant.

Logit Ensemble with Server-Side Distillation – FedDF [14] trains the target model at the server-side using the logit ensemble method. This approach is under an assumption that a large amount of unlabeled data is already available at the server side. It also assumes the server has sufficient system resources to directly run KD. FedFTG [27] also uses the server-side KD together with a feature generator. This study does not consider the system heterogeneity nor the additional unlabeled data.

Logit Ensemble, Server-Side Distillation, and Heterogeneous Models – FedGKT [28] allows the server to have its own classifier layers and train them using KD. This approach achieves promising model accuracy, however, it does not take the public data into account. FedGEMS [29] also runs KD to train a large model at the server-side. Likely to FedMD, this method also assumes the public data to be labeled. More recently, Fed-ET [15] has been proposed, which utilizes model transfer as well as weighted ensemble at the server-side. However, this approach also performs KD on the server side, and the server-side model cannot directly learn from the clients’ private data.

3 Method

We begin with an ablation study to demonstrate how logit ensemble can harm KD performance in general FL environments. Based on this analysis, we develop our novel on-device KD-based FL method, which maximizes KD performance by fully utilizing the system resources of heterogeneous devices.

3.1 Limitations of Logit Ensemble in Federated Learning Environments

Many existing works employ the logit ensemble method to implement communication-efficient online KD in FL environments [12, 13, 14, 15]. However, our empirical study finds that it can significantly hurt the model accuracy. Our research is strongly motivated by this ablation study result.

We compare the accuracy of logit ensemble and that of the conventional model aggregation. We use CIFAR-10 and Google Speech Command, computer vision and audio recognition benchmarks. First, the dataset is partitioned into two distinct subsets: one for training and the other for evaluating model accuracy. We further divide the training data into 100 small subsets using a label-based Dirichlet distribution ($\alpha = 0.1$) and assign one small subset to each client. Next, we conduct logit ensemble-based FL and model aggregation-based FL, and compare the accuracies they achieve. Note that the logit ensemble uses the full model, while the model aggregation uses a smaller model, with each layer containing 25% of the channels. This setting penalizes the model aggregation scheme in terms of the model’s learning capability, and we expect to see the adverse impact of the logit ensemble more clearly under this setting.

In Figure 1, the left bubble chart shows the class-wise data distribution per client, while the right side of the figure shows the learning curve comparisons. The bubble charts illustrate how non-IID the datasets are. Most clients have data from only a few classes, indicating highly non-IID conditions. Each learning curve chart shows the accuracies of five local models as well as the global model’s accuracy. The purple curve corresponds to the global model trained with the logit ensemble method, while the blue curve corresponds to the global model trained with conventional model aggregation. The gap between the global curve and the local curves quantifies the impact of each FL method.

When data is highly non-IID, the logit ensemble accuracy of the full model (purple curves) is considerably lower than the model aggregation accuracy of the small (25%) model (blue curves). *The logit ensemble forces all local models to be personalized without synchronizing model parameters.* Such personalized models lead to a significant degradation in the soft target quality in terms of generalization. Some previous works assume that labeled public data is available at the edge as a way to address this issue; however, having a large amount of labeled public data is unrealistic [26, 29]. In addition, new unlabeled data is most likely generated at the edge, and centralizing them to the server may pose privacy

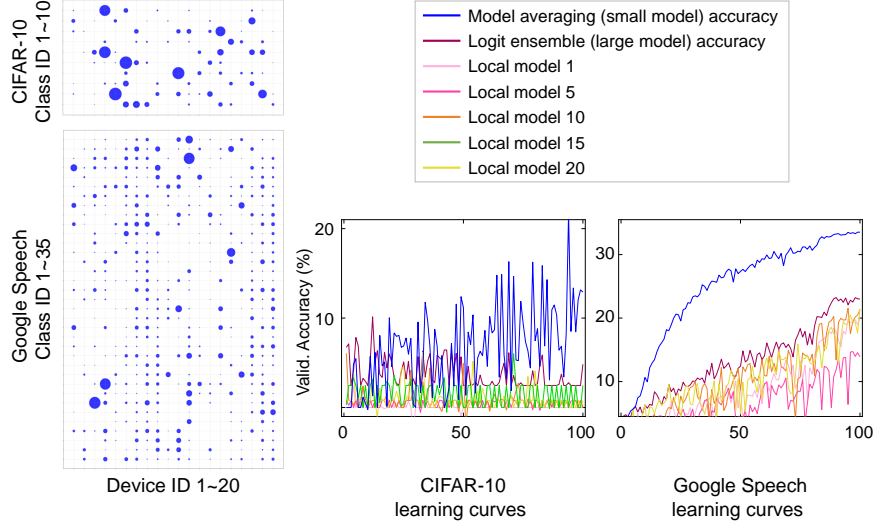


Figure 1: Non-IID distributions of CIFAR-10 (left-top) and Google Speech (left-bottom). Label-based Dirichlet distributions ($\alpha = 0.1$) are used to get 100 local distributions. Due to the limited space, we only show 20 of them. The accuracy of small model trained via FL provides remarkably more accurate logits than the logit ensemble.

concerns. For these reasons, the logit ensemble is not an appropriate option for heterogeneous FL. Motivated by this analysis, we propose a novel on-device KD-based FL method that addresses the low-quality soft target issue.

3.2 On-Device Federated Transfer Learning

We focus on federated optimization, which trains a target model \mathbf{w}_l . Considering the natural data collection at the edge, we assume that each edge device has a certain amount of unlabeled data. This is a valid problem formulation because it is more reasonable for new data to be generated at the edge rather than the parameter server. Our method employs KD with these unlabeled local data to improve the target model accuracy. We take advantage of an auxiliary model \mathbf{w}_s , which fits within the memory capacity of all individual devices. Given the two models, our method repeats the following two steps until a user-defined termination condition is satisfied (e.g., target accuracy or time budget). Figure 2 provides a schematic illustration of these two steps.

Step 1: Auxiliary Model Training Round – First, a random subset of clients is activated in each round. The activated devices receive \mathbf{w}_s from the server and run τ local updates using their own labeled data. Then, the locally trained models, \mathbf{w}_s^i for $i \in A$, are aggregated at the server, where A is the set of active clients. This global FL round with the small auxiliary model enables the collection of local knowledge from all clients, regardless of their system capacity. The loss function in step 1 is as follows.

$$\mathcal{L}_s(\mathbf{w}_s) = \frac{1}{n} \sum_{i=1}^n \text{CE}(\mathbf{w}_s, x), \forall x \in \hat{\mathcal{D}}^i, \quad (1)$$

where \mathbf{w}_s is the auxiliary model, n is the total number of clients, $\text{CE}(\cdot, \cdot)$ is the cross entropy function, and $\hat{\mathcal{D}}^i$ is the local data owned by client i .

Step 2: Target Model Training Round – Once the auxiliary models are aggregated at the server, the strong clients train the target model \mathbf{w}_l using the auxiliary model. First, the strong clients receive both models, \mathbf{w}_s and \mathbf{w}_l from the server. Then, they locally update the target model \mathbf{w}_l for τ steps using their own labeled data. After the local updates, they run additional τ local KD steps using the unlabeled local data. The auxiliary model participates in the KD process as a teacher. Finally, the local target models $\mathbf{w}_l^j, \forall j \in S$ are aggregated at the server, where S is the set of strong clients.

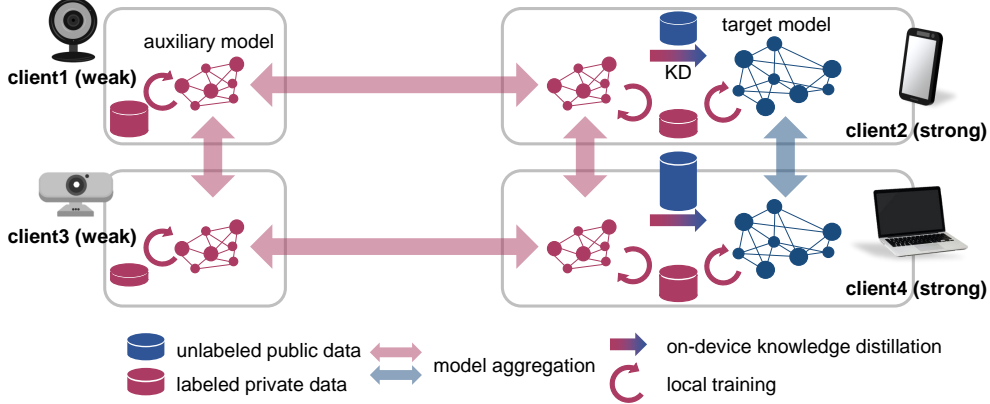


Figure 2: The schematic illustration of the proposed heterogeneous FL method. For simplicity, the server is omitted in this schematic. An auxiliary (small) model is trained by all the devices using their private data. Then, the global knowledge is transferred to the target (large) model through on-device KD. This distributed knowledge transfer approach enables to not only fully utilize heterogeneous edge devices’ system resources but also effectively use the unlabeled data for training.

In step 2, all individual strong clients train the target model \mathbf{w}_l^j using the following loss functions.

$$\begin{aligned} \mathcal{L}_l(\mathbf{w}_l) = & \frac{1}{s} \sum_{j=1}^s \text{CE}(\mathbf{w}_l, x), \forall x \in \hat{\mathcal{D}}^j \\ & + \frac{1}{s} \sum_{j=1}^s \lambda \cdot \text{KL}(\mathbf{w}_s, \mathbf{w}_l, x'), \forall x' \in \mathcal{D}^j, \end{aligned} \quad (2)$$

where \mathbf{w}_l is the target model, s is the number of strong clients, $\text{KL}(\cdot, \cdot, \cdot)$ is the Kullback–Leibler divergence function, and the λ is a hyper-parameter that determines how strongly the $\text{KL}(\cdot, \cdot, \cdot)$ affects the total loss. Note that the first term on the right-hand side uses the local labeled data $x \in \hat{\mathcal{D}}^j$ while the second term uses the local unlabeled data $x' \in \mathcal{D}^j$.

3.3 Discussion on Design Choices of On-Device Knowledge Distillation

The Role of Auxiliary Model – The core principle of our heterogeneous FL method is to use a small auxiliary model trained with a conventional model aggregation scheme. This design choice ensures local data privacy, as the auxiliary model is trained locally, and only its parameters are aggregated. In contrast, logit ensemble assumes that clients can access the same unlabeled data (also known as public data), enabling logits from different local models to be computed using the same input data. Our method does not depend on this strong assumption and allows each client to fully utilize their local data, whether labeled or unlabeled.

In addition, the logit ensemble allows local models to remain personalized, as model parameters are not directly averaged across clients. If data is highly non-IID – for example, if each client has local data limited to one or two classes – these personalized models are likely to suffer from poor generalization performance. Our ablation study shows in Figure 1. Thus, we can conclude that aggregating local logits alone is insufficient to provide accurate soft targets for KD.

Comparison to Server-side Knowledge Distillation – Our on-device KD method has three advantages over conventional server-side distillation. First, it enables the target model to utilize both labeled and unlabeled data on the clients. This is a critical benefit in terms of scalability, as the target model can learn from more unlabeled data as the number of strong clients grows. In other words, our method is better suited for on-device learning, where new data is continuously generated at the edge. Second, our method takes advantage of system heterogeneity, allowing clients with stronger system resources to run more training and distillation steps than others. This approach naturally maximizes system utilization at the edge. Finally, our method enables each client to locally utilize new data collected at runtime without sharing it with others. Some logit ensemble-based KD methods [14, 15, 29] assume that ‘public data’ are accessible at both clients and server. Such an assumption is overly strong and unrealistic, as it may pose privacy issues.

Communication Cost Analysis – We compare the communication cost of our method with that of representative logit ensemble-based KD methods. Table 2 shows the results of the comparative study using CIFAR-10 (ResNet20). FedDF employs server-side KD, whereas DS-FL adopts client-side KD. To ensure a fair comparison, we align the total number of rounds, regardless of whether they involve training or KD.

Table 2: The communication cost comparison across different FL methods. C is the number of classes. w_l is ResNet20 while w_s is a modified one which has only 25% channels at every layer.

Method	Comm. Cost	Message Size	Acc (%)
FedAvg(small)	$ w_s $	19K	$42.22 \pm 0.1\%$
FedAvg(large)	$ w_l $	274K	$59.21 \pm 1.5\%$
FedDF(small)	$ w_s $	19K	$41.62 \pm 0.1\%$
FedDF(large)	$ w_l $	274K	$59.04 \pm 0.1\%$
DS-FL	C	10	$25.95 \pm 0.1\%$
On-Device KD	$ w_s + w_l $	19K + 274K	$62.43 \pm 0.1\%$

For the homogeneous FL methods (FedAvg and FedDF), we consider two cases: one case is when the small model w_s (with 25% of the channels at every layer) is trained on all clients, and the other case is when the large model w_l is trained only on a subset of clients with sufficiently strong system resources. First, FedAvg (small) has a lower communication cost than FedAvg (large), but suffers from significantly lower accuracy. Interestingly, the accuracy of FedDF is lower than that of FedAvg, regardless of the model size. This result indicates that the soft targets generated by the logit ensemble are of insufficient quality to make meaningful progress in KD. FedDF can leverage KD without incurring extra communication cost. However, it runs KD on the server-side with inaccurate soft targets, which could ultimately harm model accuracy. DS-FL, the client-side KD-based FL method, adopts the logit ensemble and entirely avoids the model aggregation cost. Thus, the communication cost is only the number of classes C , but the model accuracy is significantly reduced.

The communication cost of our method is slightly higher than that of FedAvg(large) due to the extra communication for the auxiliary model training. However, the accuracy improves remarkably, even surpassing that of FedAvg (large). This analysis demonstrates that our method strikes a practical trade-off between communication cost and model accuracy.

3.4 Discussion on Impact of On-Device Knowledge Distillation on Generalization Performance

Here, we analyze the benefit of our design choices in terms of the target model’s generalization bound. Our analysis builds upon that of [15], extending it to account for the combination of labeled and unlabeled local data.

Problem Definition – We first define hypothesis $h : \mathcal{X} \rightarrow \mathcal{Y}$, with input space $\mathbf{x} \in \mathcal{X}$ and label space $y \in \mathcal{Y}$, and the hypothesis space \mathcal{H} . The general loss function $l(h(\mathbf{x}), y)$ quantifies the classification error of the given hypothesis. The true global data distribution is defined as \mathcal{D} . Then, the true local data distribution from each client’s perspective is defined as $\mathcal{D}_i, i \in [n]$. The data distribution of the limited number of local observations is defined as $\hat{\mathcal{D}}_i$. We also define the expected loss over an arbitrary data distribution \mathcal{D}' as $\mathcal{L}_{\mathcal{D}'}(h) = \mathbb{E}_{\mathbf{x}, y \sim \mathcal{D}'} [l(h(\mathbf{x}), y)], \forall h \in \mathcal{H}$. Finally, we assume that $\mathcal{L}(h)$ is convex. In these settings, the generalization bound of the target model trained by our proposed method satisfies the following condition.

To make our analysis self-contained, we state the two lemmas proposed in the previous work, which will be used to analyze the generalization of our proposed method.

Lemma 1 (Domain Adaptation) [30].

With two true distributions \mathcal{D}_1 and $\mathcal{D}_2, \forall p \in (0, 1)$ and hypothesis $\forall h \in \mathcal{H}$, with probability at least $1 - p$ over the choice of samples, it satisfies

$$\mathcal{L}_{\mathcal{D}_1}(h) \leq \mathcal{L}_{\mathcal{D}_2}(h) + \frac{1}{2}d(\mathcal{D}_1, \mathcal{D}_2) + v, \quad (3)$$

where $d(\mathcal{D}_1, \mathcal{D}_2)$ quantifies the distribution discrepancy between the two data distributions, \mathcal{D}_1 and \mathcal{D}_2, v_i is the minimal loss such that $v_i = \inf_h \mathcal{L}_{\mathcal{D}_i}(h) + \mathcal{L}_{\mathcal{D}}(h)$.

Lemma 2 (Generalization with limited training samples) [15]. For all individual client i , with probability at least $1 - p$ over the choice of samples, there exists:

$$\mathcal{L}_{\mathcal{D}_i}(h_{\hat{\mathcal{D}}_i}) \leq \mathcal{L}_{\hat{\mathcal{D}}_i}(h_{\hat{\mathcal{D}}_i}) + \sqrt{\frac{\log 2/p}{2|\hat{\mathcal{D}}_i|}}, \quad (4)$$

where $|\hat{\mathcal{D}}_i|$ is the size of client i ’s local dataset.

The first lemma provides a generalization bound for one data distribution based on the maximum discrepancy between the two given distributions. The second lemma refines this bound by considering the limited training samples, leveraging Hoeffding’s inequality. Our proposed method trains the target model \mathbf{x}_l using only $s < n$ strong clients. Accordingly, we analyze the generalization bound with respect to the labeled data from the strong clients using the two lemmas above. Subsequently, we revise this bound to incorporate on-device KD with unlabeled local data. See Appendix for proof.

Dataset	Batch (LR)	Local Steps	Epochs	# of clients	Weak-only	Strong-only	Proposed
CIFAR-10	32 (0.2)	30	400	100	49.11 ± 0.1%	59.21 ± 1.5%	62.43 ± 0.1%
FEMNIST	20 (0.02)	30	200	100	64.19 ± 0.1%	53.75 ± 0.6%	67.44 ± 0.1%
CIFAR-100 (Fine-tuning)	32 (0.04)	60	40	100	40.56 ± 0.1%	52.17 ± 0.1%	59.73 ± 0.1%
IMDB review	10 (0.4)	20	90	50	81.46 ± 0.1%	59.63 ± 0.1%	82.50 ± 0.1%
Google Speech	32 (0.02)	40	100	100	66.83 ± 0.3%	68.83 ± 0.1%	71.95 ± 0.5%

Table 3: The FL performance comparison: weak model-only, strong model-only and the proposed method.

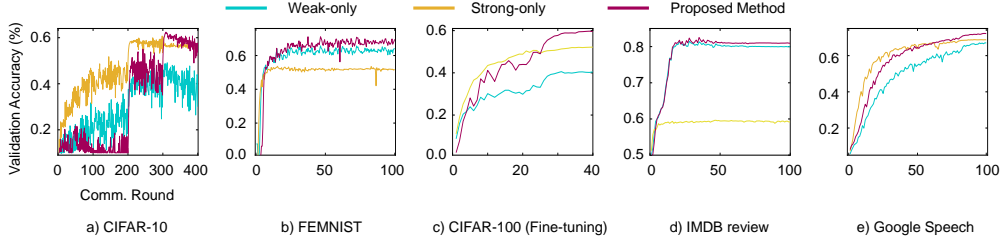


Figure 3: The validation accuracy curves corresponding to Table 3.

Proposition 1 Consider n clients in total and s of them are strong clients. Each client has its own data distribution $\mathcal{D}_i, \forall i \in [n]$. We define a combination of the labeled local data and the unlabeled local data as $\tilde{\mathcal{D}}_i$. For an arbitrary data distribution \mathcal{D}' , $h_{\mathcal{D}'}$ is the model best-trained on \mathcal{D}' . Then, with probability of $1 - p$, our proposed on-device KD-based FL guarantees the following generalization bound for the target model.

$$\mathcal{L}_{\mathcal{D}} \left(\frac{1}{s} \sum_{i=1}^s h_{\tilde{\mathcal{D}}_i} \right) \leq \frac{1}{s} \sum_{i=1}^s \left(\mathcal{L}_{\tilde{\mathcal{D}}_i} (h_{\tilde{\mathcal{D}}_i}) + \sqrt{\frac{\log 2/p}{2|\tilde{\mathcal{D}}_i|}} \right) + \frac{1}{2s} \sum_{i=1}^s d(\mathcal{D}_i, \mathcal{D}) + \frac{1}{s} \sum_{i=1}^s v_i.$$

Remark 1. This result shows the key advantage of our method: The on-device KD reduces the second term on the right-hand side in (6), which means better generalization. Remember that $|\hat{\mathcal{D}}_i| \leq |\tilde{\mathcal{D}}_i|$, where $\hat{\mathcal{D}}_i$ is the labeled data and $\tilde{\mathcal{D}}_i$ is the combination of labeled and unlabeled data. Thus, we can expect that the proposed method achieves a lower empirical loss by enlarging the data distribution.

Remark 2. As each client collects more unlabeled data, the size of $\tilde{\mathcal{D}}_i$ grows, and the bound becomes even smaller. This is a crucial benefit in realistic FL environments, as new unlabeled data is most likely collected at the edge rather than the server. So, our method can be considered as a more scalable FL method especially when the strong clients can collect data on-the-fly. Note that in the server-side KD, the $\hat{\mathcal{D}}_i$ can only be the unlabeled data which is still smaller than $\tilde{\mathcal{D}}_i$.

4 Experiments

We conduct performance evaluations with computer vision: CIFAR-10 (ResNet20 [31]), CIFAR-100 (ViT [32]), FEMNIST (CNN), natural language processing: IMDB (Bidirectional LSTM), and audio recognition: Google Speech Command (CNN) benchmarks. We report accuracy averaged across at least 3 independent runs. For all the methods in our comparative study, the algorithm-specific hyper-parameters were highly tuned using appropriate grid searches. See Appendix for the hyper-parameter settings in detail.

Non-IID Dataset Settings – We use label-based Dirichlet distributions ($\alpha = 0.1$ which represents highly non-IID FL environments). FEMNIST is naturally non-IID, and we use 100 clients’ data as unlabeled local data. Google Speech is also naturally non-IID, but each local dataset is quite large. So, we use an artificial distribution to make it more strongly non-IID. We activate random 20% of the total clients at every round. In all our experiments, a half of dataset is distributed to all clients as unlabeled local data.

4.1 Performance Evaluation

We first define ‘weak’ and ‘strong’ clients based on their system capability. Here, *weak* client indicates the devices that have insufficient system resources to train the large target model. The *strong* client is the devices that have system

Dataset	Auxiliary Model (<i>weak</i>) (relative model size)	Target Model (<i>strong</i>)
CIFAR-10	ResNet20 {25%, 50%, 75%}	ResNet20 100%
FEMNIST	CNN {25%, 50%, 75%}	CNN 100%
CIFAR-100 (Fine-tuning)	ResNet50 ~ 29%	ViT-b16 100%
IMDB	Bi-LSTM 25%	Bi-LSTM 100%
Google Speech	CNN {25%, 50%, 75%}	CNN 100%

Table 4: The model configurations for all five benchmarks.

Dataset	FedAvg (homo)	MOON (homo)	FedDF (homo)	DS-FL (hetero)	FedMD (hetero)	FedGEM (hetero)	Proposed (hetero)
Public Data	N/A	N/A	Unlabeled	Unlabeled	Labeled	Labeled	Unlabeled
CIFAR-10	57.98 ± 0.3%	58.38 ± 0.1%	58.84 ± 0.1%	25.95 ± 0.1%	61.13 ± 0.1%	34.27 ± 0.1%	62.43 ± 0.1%
FEMNIST	64.27 ± 0.1%	64.80 ± 0.1%	66.90 ± 0.2%	56.71 ± 0.5%	65.23 ± 0.1%	65.06 ± 0.1%	67.44 ± 0.1%
Google Speech	66.05 ± 0.7%	N/A	59.58 ± 0.2%	19.14 ± 0.1%	65.90 ± 0.1%	25.20 ± 0.2%	71.95 ± 0.5%

Table 5: The FL performance comparison across SOTA KD-based FL methods. 20% of the total clients are *strong* clients and the auxiliary model size is 25% of the target model. Our method achieves the best accuracy without extra labeled data (public data). MOON is designed only for image data, and thus we do not apply it to Google Speech, the audio benchmark.

resources strong enough to train the full target model. For extensive empirical study, we use a variety of different *weak* clients as shown in Table 4.

Table 3 shows the performance comparison between two baselines and the proposed method, and Figure 3 shows the corresponding validation accuracy curves (See Appendix for the loss curves). We consider two baselines: *weak-only*, where the model size is reduced to fit within all clients’ memory space and *strong-only*, where the *weak* clients are excluded and only the *strong* clients participate in the large model training. These two baselines are the most straightforward options for standard FL. By comparing our method to these two baselines, we can evaluate how well the proposed on-device KD utilizes the *weak* clients’ local data to strengthen the large target model. To ensure a fair comparison in terms of computational cost, the *strong-only* method performs 2τ local steps, while our method runs τ local SGD steps and τ KD steps.

Table 3 shows that the proposed method remarkably improves the target model accuracy. The performance gap mainly comes from the knowledge transferred from the auxiliary model which learns from all clients’ local data. The same result can be observed across different applications, computer vision benchmarks and audio command detection benchmark. It also works well with the transformer-based fine-tuning task. Therefore, we can conclude that the proposed method effectively improves the large model’s performance by utilizing many *weak* clients’ local data.

4.2 Comparative Study

We compare our method to three homogeneous FL methods: FedAvg, MOON, and FedDF, and heterogeneous FL methods: DS-FL, FedMD, and FedGEM [29] as shown in Table 5. The homogeneous FL methods use a small model that has 25% of channels at each layer. The heterogeneous FL methods use the full model at 20% of the clients and the small model at the rest of the clients. These settings well represent the realistic FL environments consisting of edge devices with heterogeneous system resources.

We do not compare our method to FedGKT [28] and Fed-ET [15] since they are composed of several features independent of KD. E.g., their representation transfer can be applied to our method without any conflicts. We also do not present time vs. accuracy results because all the methods have a different computation to communication ratio per round. Our study instead focuses on the achievable accuracy within a sufficiently large epoch budget.

Comparison to Homogeneous FL Methods – MOON achieves higher accuracy than FedAvg showing a practical use-case of contrastive loss. FedDF achieves even higher accuracy than MOON thanks to its server-side KD with public data. However, because these methods do not consider the system heterogeneity, they cannot train large models that do not fit into weak clients’ memory space. In contrast, our method can train large target models achieving superior performance by exploiting the strong clients’ system resources.

Comparison to Heterogeneous FL Methods – DS-FL shows much lower accuracy than others due to the personalized local models. This result is well aligned with our ablation study shown in Figure 1 such that the logit ensemble harms the soft target quality dramatically losing the accuracy. FedMD achieves much higher accuracy than DS-FL. However, the performance gain mainly comes from the labeled public data shared across all the clients. In addition, FedMD is not applicable to the environments where the unlabeled data is distributed to the edge since the global logit should be calculated from the local logits obtained from the same data across all the clients. FedGEM achieves inconsistent performance across benchmarks. Due to the poor soft target quality caused by the logit ensemble, it severely loses the accuracy. FedGEM also assumes the labeled public data like FedMD, which is not realistic. Based on this comparative study, we can conclude that our method utilizes the unlabeled data more effectively than other methods.

5 Conclusion

We proposed a novel on-device KD-based heterogeneous FL method. Our method exploits the heterogeneous system resources at the edge via local KD with periodic model aggregations. This approach enables the target model to learn from the local data regardless of whether they are labeled or not. This is the key advantage as it will allow FL applications to leverage the continuously generated local data at the edge without needing to share it across clients. Our study demonstrates that the proposed on-device KD method also effectively improves the knowledge transfer efficiency even under extremely non-IID environments. More importantly, our study empirically proves that the large model can be well trained on the distributed non-IID data without relying on the server-side resources or the centralized public data. We believe that harmonizing our method and the communication-efficient model aggregation methods is critical future work.

References

- [1] Brendan McMahan, Eider Moore, Daniel Ramage, Seth Hampson, and Blaise Aguera y Arcas. Communication-efficient learning of deep networks from decentralized data. In *Artificial intelligence and statistics*, pages 1273–1282. PMLR, 2017.
- [2] Qiong Chen, Zimu Zheng, Chuang Hu, Dan Wang, and Fangming Liu. On-edge multi-task transfer learning: Model and practice with data-driven task allocation. *IEEE Transactions on Parallel and Distributed Systems*, 31(6):1357–1371, 2019.
- [3] Ziqing Fan, Shengchao Hu, Jiangchao Yao, Gang Niu, Ya Zhang, Masashi Sugiyama, and Yanfeng Wang. Locally estimated global perturbations are better than local perturbations for federated sharpness-aware minimization. In *International Conference on Machine Learning*, volume 235, pages 12858–12881, 2024.
- [4] Ligeng Zhu, Lanxiang Hu, Ji Lin, Wei-Ming Chen, Wei-Chen Wang, Chuang Gan, and Song Han. Pockengine: Sparse and efficient fine-tuning in a pocket. In *Proceedings of the 56th Annual IEEE/ACM International Symposium on Microarchitecture*, pages 1381–1394, 2023.
- [5] Enmao Diao, Jie Ding, and Vahid Tarokh. Heterofl: Computation and communication efficient federated learning for heterogeneous clients. *arXiv preprint arXiv:2010.01264*, 2020.
- [6] Samuel Horvath, Stefanos Laskaridis, Mario Almeida, Ilias Leontiadis, Stylianos Venieris, and Nicholas Lane. Fjord: Fair and accurate federated learning under heterogeneous targets with ordered dropout. *Advances in Neural Information Processing Systems*, 34:12876–12889, 2021.
- [7] Sunwoo Lee, Tuo Zhang, and A Salman Avestimehr. Layer-wise adaptive model aggregation for scalable federated learning. In *Proceedings of the AAAI Conference on Artificial Intelligence*, volume 37, pages 8491–8499, 2023.
- [8] Sunwoo Lee, Anit Kumar Sahu, Chaoyang He, and Salman Avestimehr. Partial model averaging in federated learning: Performance guarantees and benefits. *Neurocomputing*, 556:126647, 2023.
- [9] Sunwoo Lee, Tuo Zhang, Saurav Prakash, Yue Niu, and Salman Avestimehr. Embracing federated learning: Enabling weak client participation via partial model training. *IEEE Transactions on Mobile Computing*, 2024.
- [10] Tuo Zhang, Lei Gao, Sunwoo Lee, Mi Zhang, and Salman Avestimehr. Timelyfl: Heterogeneity-aware asynchronous federated learning with adaptive partial training. In *Proceedings of the IEEE/CVF Conference on Computer Vision and Pattern Recognition*, pages 5064–5073, 2023.
- [11] Geoffrey Hinton, Oriol Vinyals, and Jeff Dean. Distilling the knowledge in a neural network. *arXiv preprint arXiv:1503.02531*, 2015.
- [12] Eunjeong Jeong, Seungeun Oh, Hyesung Kim, Jihong Park, Mehdi Bennis, and Seong-Lyun Kim. Communication-efficient on-device machine learning: Federated distillation and augmentation under non-iid private data. *arXiv preprint arXiv:1811.11479*, 2018.

- [13] Sohei Itahara, Takayuki Nishio, Yusuke Koda, Masahiro Morikura, and Koji Yamamoto. Distillation-based semi-supervised federated learning for communication-efficient collaborative training with non-iid private data. *IEEE Transactions on Mobile Computing*, 22(1):191–205, 2021.
- [14] Tao Lin, Lingjing Kong, Sebastian U Stich, and Martin Jaggi. Ensemble distillation for robust model fusion in federated learning. *Advances in neural information processing systems*, 33:2351–2363, 2020.
- [15] Yae Jee Cho, Andre Manoel, Gauri Joshi, Robert Sim, and Dimitrios Dimitriadis. Heterogeneous ensemble knowledge transfer for training large models in federated learning. *arXiv preprint arXiv:2204.12703*, 2022.
- [16] Alex Krizhevsky, Geoffrey Hinton, et al. Learning multiple layers of features from tiny images. 2009.
- [17] Sebastian Caldas, Peter Wu, Tian Li, Jakub Konečný, H Brendan McMahan, Virginia Smith, and Ameet Talwalkar. Leaf: A benchmark for federated settings. *arXiv preprint arXiv:1812.01097*, 2018.
- [18] Aditya Pal, Abhilash Barigidad, and Abhijit Mustafi. Imdb movie reviews dataset, 2020.
- [19] Pete Warden. Speech commands: A dataset for limited-vocabulary speech recognition. *arXiv preprint arXiv:1804.03209*, 2018.
- [20] Samiul Alam, Luyang Liu, Ming Yan, and Mi Zhang. Fedrolex: Model-heterogeneous federated learning with rolling sub-model extraction. *Advances in neural information processing systems*, 35:29677–29690, 2022.
- [21] Dezhong Yao, Wanning Pan, Michael J O’Neill, Yutong Dai, Yao Wan, Hai Jin, and Lichao Sun. Fedhm: Efficient federated learning for heterogeneous models via low-rank factorization. *arXiv preprint arXiv:2111.14655*, 2021.
- [22] Jiaqi Liu, Kaiyu Huang, and Lunchen Xie. Hetefed: Heterogeneous federated learning with privacy-preserving binary low-rank matrix decomposition method. In *2023 26th International Conference on Computer Supported Cooperative Work in Design (CSCWD)*, pages 1238–1244. IEEE, 2023.
- [23] Yun Hin Chan and Edith CH Ngai. Fedhe: Heterogeneous models and communication-efficient federated learning. In *2021 17th International Conference on Mobility, Sensing and Networking (MSN)*, pages 207–214. IEEE, 2021.
- [24] Yue Niu, Saurav Prakash, Souvik Kundu, Sunwoo Lee, and Salman Avestimehr. Federated learning of large models at the edge via principal sub-model training. *arXiv preprint arXiv:2208.13141*, 2022.
- [25] Qinbin Li, Bingsheng He, and Dawn Song. Model-contrastive federated learning. In *Proceedings of the IEEE/CVF conference on computer vision and pattern recognition*, pages 10713–10722, 2021.
- [26] Daliang Li and Junpu Wang. Fedmd: Heterogenous federated learning via model distillation. *arXiv preprint arXiv:1910.03581*, 2019.
- [27] Lin Zhang, Li Shen, Liang Ding, Dacheng Tao, and Ling-Yu Duan. Fine-tuning global model via data-free knowledge distillation for non-iid federated learning. In *Proceedings of the IEEE/CVF conference on computer vision and pattern recognition*, pages 10174–10183, 2022.
- [28] Chaoyang He, Murali Annavam, and Salman Avestimehr. Group knowledge transfer: Federated learning of large cnns at the edge. *Advances in Neural Information Processing Systems*, 33:14068–14080, 2020.
- [29] Sijie Cheng, Jingwen Wu, Yanghua Xiao, and Yang Liu. Fedgems: Federated learning of larger server models via selective knowledge fusion. *arXiv preprint arXiv:2110.11027*, 2021.
- [30] Shai Ben-David, John Blitzer, Koby Crammer, Alex Kulesza, Fernando Pereira, and Jennifer Wortman Vaughan. A theory of learning from different domains. *Machine learning*, 79:151–175, 2010.
- [31] Kaiming He, Xiangyu Zhang, Shaoqing Ren, and Jian Sun. Deep residual learning for image recognition. In *Proceedings of the IEEE conference on computer vision and pattern recognition*, pages 770–778, 2016.
- [32] Alexey Dosovitskiy, Lucas Beyer, Alexander Kolesnikov, Dirk Weissenborn, Xiaohua Zhai, Thomas Unterthiner, Mostafa Dehghani, Matthias Minderer, Georg Heigold, Sylvain Gelly, et al. An image is worth 16x16 words: Transformers for image recognition at scale. *arXiv preprint arXiv:2010.11929*, 2020.
- [33] Guile Wu and Shaogang Gong. Peer collaborative learning for online knowledge distillation. In *Proceedings of the AAAI Conference on artificial intelligence*, volume 35, pages 10302–10310, 2021.

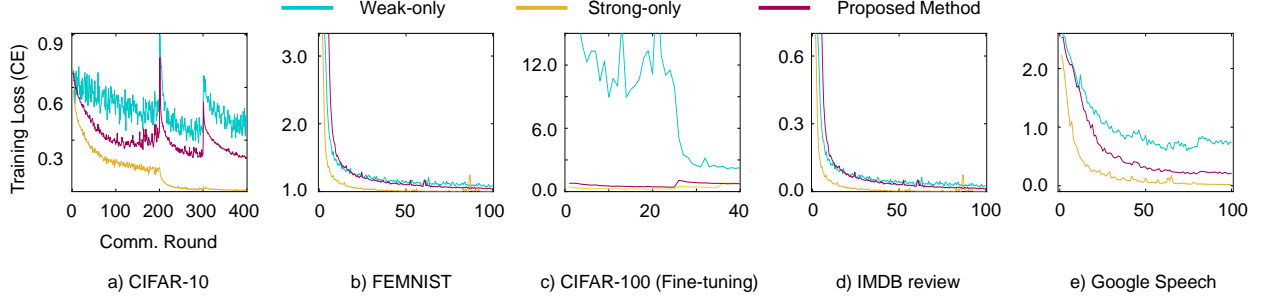


Figure 4: The training loss curves corresponding to Table 3.

6 Appendix

6.1 Additional Experimental Results

We use TensorFlow 2.13.0 and MPI (OpenMPI 4.1.5) for FL simulation. All experiments run on a GPU cluster that contains 2 NVIDIA A6000 GPUs. For all the methods in our comparative study, the algorithm-specific hyper-parameters were highly tuned using appropriate grid searches (See Appendix for the details). For CIFAR-100 fine-tuning, we freeze the transformer pre-trained on ImageNet and train the output-side two fully-connected layers only.

The loss curve comparisons corresponding to Table 5 is shown in Figure 4. We see the same patterns in the accuracy curves shown in Figure 3.

6.2 Proof of Proposition 1

Proposition 1 Consider n clients in total and s of them are strong clients. Each client has its own data distribution $\mathcal{D}_i, \forall i \in [n]$. We define a combination of the labeled local data and the unlabeled local data as $\hat{\mathcal{D}}_i$. For an arbitrary data distribution \mathcal{D}' , $h_{\mathcal{D}'}$ is the model best-trained on \mathcal{D}' . Then, with probability of $1 - p$, our proposed on-device knowledge distillation-based FL guarantees the following generalization bound for the target model.

$$\begin{aligned} \mathcal{L}_{\mathcal{D}} \left(\frac{1}{s} \sum_{i=1}^s h_{\hat{\mathcal{D}}_i} \right) &\leq \frac{1}{s} \sum_{i=1}^s \left(\mathcal{L}_{\hat{\mathcal{D}}_i} (h_{\hat{\mathcal{D}}_i}) + \sqrt{\frac{\log 2/p}{2|\hat{\mathcal{D}}_i|}} \right) \\ &\quad + \frac{1}{2s} \sum_{i=1}^s d(\mathcal{D}_i, \mathcal{D}) + \frac{1}{s} \sum_{i=1}^s v_i. \end{aligned}$$

Proof. First, let us bound the loss over the true global data distribution $\mathcal{L}_{\mathcal{D}}(\frac{1}{s} \sum_{i=1}^s h_{\hat{\mathcal{D}}_i})$ based on lemma 1. Note that the hypothesis is the model averaged only across s strong clients.

$$\begin{aligned} \mathcal{L}_{\mathcal{D}} \left(\frac{1}{s} \sum_{i=1}^s h_{\hat{\mathcal{D}}_i} \right) &\leq \frac{1}{s} \sum_{i=1}^s \mathcal{L}_{\mathcal{D}} (h_{\hat{\mathcal{D}}_i}) \\ &\leq \frac{1}{s} \sum_{i=1}^s \left(\mathcal{L}_{\mathcal{D}_i} (h_{\hat{\mathcal{D}}_i}) + \frac{1}{2} d(\mathcal{D}_i, \mathcal{D}) + v_i \right). \end{aligned} \tag{5}$$

Then, (5) can be further bounded using lemma 2 as follows.

$$\begin{aligned} \mathcal{L}_{\mathcal{D}} \left(\frac{1}{s} \sum_{i=1}^s h_{\hat{\mathcal{D}}_i} \right) &\leq \frac{1}{s} \sum_{i=1}^s \left(\mathcal{L}_{\hat{\mathcal{D}}_i} (h_{\hat{\mathcal{D}}_i}) + \sqrt{\frac{\log 2/p}{2|\hat{\mathcal{D}}_i|}} \right) \\ &\quad + \frac{1}{2s} \sum_{i=1}^s d(\mathcal{D}_i, \mathcal{D}) + \frac{1}{s} \sum_{i=1}^s v_i. \end{aligned}$$

Finally, the on-device knowledge distillation utilizes not only the strong clients’ labeled data but also the unlabeled data. Thus, we can simply replace the local dataset $\hat{\mathcal{D}}_i$ with the combination of the labeled and unlabeled data $\tilde{\mathcal{D}}_i$.

$$\begin{aligned} \mathcal{L}_{\mathcal{D}} \left(\frac{1}{s} \sum_{i=1}^s h_{\hat{\mathcal{D}}_i} \right) &\leq \frac{1}{s} \sum_{i=1}^s \left(\mathcal{L}_{\tilde{\mathcal{D}}_i} (h_{\tilde{\mathcal{D}}_i}) + \sqrt{\frac{\log 2/p}{2|\tilde{\mathcal{D}}_i|}} \right) \\ &\quad + \frac{1}{2s} \sum_{i=1}^s d(\mathcal{D}_i, \mathcal{D}) + \frac{1}{s} \sum_{i=1}^s v_i. \end{aligned} \quad (6)$$

□

6.3 Data Preprocessing

Some benchmark datasets require a couple of preprocessing steps so that the model can effectively learn meaningful knowledge.

CIFAR-10, CIFAR-100 – We perform the typical image preprocessing used in many previous works. First, each image is padded by 4 pixels on every dimension and then randomly cropped to the original size. Then, we normalize and standardize the values for all individual pixels. Finally, we randomly flip the image horizontally with probability of 0.5.

Google Speech Command – We apply a few audio preprocessing steps to each *wav* file. First, the raw data is decoded and read into the memory space. Second, we zero out all the values that lie below 18,000 samples (1 sec). Finally, we apply short-time fourier transform to the data to get spectrogram. In this way, each wav file becomes a 2-D spectrogram matrix that can be directly injected to the model for training.

6.4 Algorithm-Specific Hyper-Parameter Settings

To improve the reproducibility, we provide the detailed hyper-parameter settings we used when measuring the SOTA algorithms’ FL performance. We summarize the hyper-parameter settings corresponding to Table 3 in Tables 6 to 10. The hyper-parameter settings corresponding to Table 5 are shown in Tables 11 to 13.

Homogeneous FL methods – For the algorithms that do not run KD (FedAvg and MOON), the number of local steps is set to 2τ while all the others run τ SGD steps and then τ KD steps. Although it does not guarantee exactly the same computational cost across the algorithms, it allows them to have similar workload at least. MOON is an advanced FL optimization algorithm that redesigns the loss function to address the data heterogeneity issue. However, it is designed only for computer vision tasks, and thus we evaluate its performance and compare to our method in computer vision benchmarks only.

FedMD – When running FedMD, we found that the transfer learning with private data achieves better accuracy when the learning rate is much smaller than the training with public data. Thus, we do not re-initialize the learning rate after the learning rate decay in the transfer learning with public data and just use the small learning rate during the transfer learning with private data.

FedGEM – FedGEM has a weight factor ϵ which determines how much KL contribute to the total loss. We set ϵ to 0.75 as the original authors presented in [29]. FedGEM also uses a relatively smaller number of local steps τ compared to other SOTA algorithms. Because FedGEM has three training rounds in total, two at the edge and one at the server-side, we set the τ to make the total steps the same as other algorithms. For example, in FEMNIST experiments, FedAvg runs 60 steps, FedDF runs 30 SGD steps + 30 KD steps, and FedGEM runs 20 + 20 client steps and 20 server steps. While conducting experiments with FedGEM and DS-FL on the CIFAR-10, we observed that decaying the learning rate does not result in any significant changes in accuracy. Therefore, we use a fixed learning rate without decay.

Proposed Method – We found that a small KL coefficient λ helps improve our method accuracy. Instead of using a constant setting, we employed a structured coefficient control method proposed in [33]. We applied this to other SOTA methods, however, we have not observed any meaningful accuracy improvements.

Table 6: CIFAR-10 Hyper-Parameter Settings

Hyperparameters	Weak-only	Strong - only	Proposed
model size	25%	100%	100%
τ (local steps)	30	60	30
batch size		32	
learning rate	0.2, 0.02(200 epoch), 0.002(300 epoch)		
total epoch	400		
weight decay	0.0001		
temperature	3		
epoch threshold for λ ramp-up	300		
λ (KL coefficient)	0.5		
α (Dirichlet coefficient)	0.1		

Table 7: FEMNIST Hyper-Parameter Settings

Hyperparameters	Weak-only	Strong - only	Proposed
model size	25%	100%	100%
τ (local steps)	30	60	30
batch size		20	
learning rate		0.02	
total epoch		200	
weight decay		0.0001	
temperature		3	
λ (KL coefficient)		1	
α (Dirichlet coefficient)		0.1	

Table 8: CIFAR-100 (Fine-tuning) Hyper-Parameters

Hyperparameters	Weak-only	Strong - only	Proposed
model	ResNet50	ViT-b16	ViT-b16
τ (local steps)	60	120	60
batch size		32	
learning rate	0.04, 0.004(25 epoch), 0.0004(35 epoch)		
total epoch	40		
weight decay	0.0005		
temperature	1		
λ (KL coefficient)	1		
α (Dirichlet coefficient)	0.1		

Table 9: IMDB review Hyper-Parameter Settings

Hyperparameters	Weak-only	Strong - only	Proposed
model size	25%	100%	100%
τ (local steps)	20	40	20
batch size		10	
learning rate		0.4	
total epoch		90	
weight decay		0.0001	
temperature		1	
epoch threshold for λ ramp-up		80	
λ (KL coefficient)		1	
α (Dirichlet coefficient)		0.1	

Table 10: Google Speech Hyper-Parameter Settings

Hyperparameters	Weak-only	Strong - only	Proposed
model size	25%	100%	100%
τ (local steps)	40	80	40
batch size		32	
learning rate	0.02, 0.002 (80 epoch)		
total epoch	100		
weight decay	0.0001		
temperature	1		
epoch threshold for λ ramp-up	80		
λ (KL coefficient)	1		
α (Dirichlet coefficient)	0.1		

Table 11: CIFAR-10 Hyper-Parameter Settings for SOTA FL Methods

Hyperparameters	FedAvg	MOON	FedDF	DS-FL	FedMD	FedGEM	Proposed
client model size	25%	25%	25%	80 clients: 25% 20 clients: 100%	80 clients: 25% 20 clients: 100%	80 clients: 25% 20 clients: 100%	80 clients: 25% 20 clients: 100%
server model size	25%	25%	25%	N/A	N/A	100%	N/A
τ (local steps)	60	60	30	30	30	20	30
learning rate	0.2	0.2	0.2	0.01	0.2	0.05	0.2
temperature	N/A	N/A	1	1	1	1	3
batch size					32		
total epoch					400		
weight decay					0.0001		

Table 12: FEMNIST Hyper-Parameter Settings for SOTA FL Methods

Hyperparameters	FedAvg	MOON	FedDF	DS-FL	FedMD	FedGEM	Proposed
client model size	25%	25%	25%	80 clients: 25% 20 clients: 100%	80 clients: 25% 20 clients: 100%	80 clients: 25% 20 clients: 100%	80 clients: 25% 20 clients: 100%
server model size	25%	25%	25%	N/A	N/A	100%	N/A
τ (local steps)	60	60	30	30	30	20	30
learning rate	0.02	0.02	0.01	0.01	0.01	0.01	0.02
temperature	N/A	N/A	1	1	1	1	3
batch size					20		
total epoch					200		
weight decay					0.0001		

Table 13: Google Speech Hyper-Parameter Settings for SOTA FL Methods

Hyperparameters	FedAvg	MOON	FedDF	DS-FL	FedMD	FedGEM	Proposed
client model size	25%	N/A	25%	80 clients: 25% 20 clients: 100%	80 clients: 25% 20 clients: 100%	80 clients: 25% 20 clients: 100%	80 clients: 25% 20 clients: 100%
server model size	25%	N/A	25%	N/A	N/A	100%	N/A
τ (local steps)	80	N/A	40	40	40	30	40
learning rate	0.02	N/A	0.02	0.01	0.02	0.02	0.02
temperature					1		
batch size					32		
total epoch					100		
weight decay					0.0001		